PS Impact of Non-Linear Transport Properties on Low Permeability Measurements*

Yuan-Yun Lin[1] and Michael T. Myers[1]

Search and Discovery Article #70299 (2017)**

Posted October 23, 2017

*Adapted from poster presentation given at AAPG 2017 Annual Convention and Exhibition, Houston, Texas, United States, April 2-5, 2017

[1]University of Houston, Houston, TX, United States (uhylin41@gmail.com)

Abstract

This paper presents the results of modeling of five different plug based measurement protocols, and discusses their strength and weaknesses. The necessity of using the full nonlinear flow equation for the interpretation of the data is also discussed. Five different protocols are modeled: steady state, unsteady state, pulse decay, sinusoidal pressure and moving boundary conditions. These differ by the addition of reference chambers to the steady state apparatus and the pressure boundary conditions applied. Our implementation of the nonlinear equation includes the assumption of constant viscosity, rock compressibility, and pressure dependent permeability, i.e. the gas slippage effect (Klinkenberg corrections). We find that variable (pressure dependent) density increases the average pressure in the sample due to the nonlinear pressure profile induced. This leads to the estimation of permeability that is too small compared to an assumption of a linear profile. In contrast, the Klinkenberg effect causes an increased estimated permeability. It is difficult to separate these two effects; as a result, modeling the full nonlinear behavior of the transport properties is necessary. From the results of the modeling, we believe plug scale measurements are practical, and grinding of samples is not necessary. We recommend using unsteady state measurements, supplemented with sinusoidal pressure and pulse decay to calibrate the magnitude of the nonlinear effects, and the impact of diffusion and absorption.

References Cited

Cui, X., A.M.M. Bustin, and R.M. Bustin, 2009, Measurements of gas permeability and diffusivity of tight reservoir rocks: different approaches and their applications: Geofluids, v. 9/3, p. 208-223.

Sander, R., Z. Pan, and L.D. Connell, 2017, Laboratory measurement of low permeability unconventional gas reservoir rocks: A review of experimental methods: Journal of Natural Gas Science and Engineering, v. 37, p. 248-279.

Darcy, H., 1856, Les fontaines publiques de la ville de Dijon: exposition et application... Victor Dalmont.

Klinkenberg, L.J., 1941, The permeability of porous media to liquids and gases: Drilling and production practice, American Petroleum Institute.

Aronofsky, J.S., 1954, Effect of gas slip on unsteady flow of gas through porous media: Journal of Applied Physics, v. 25/1, p. 48-53.

Profice, S., D. Lasseux, Y. Jannot, N. Jebara, and G. Hamon, 2012, Permeability, porosity and klinkenberg coefficien determination on crushed porous media: Petrophysics, v. 53/6, p. 430-438.

Fischer, G.J., 1992, The determination of permeability and storage capacity: Pore pressure oscillation method: International Geophysics, v. 51, p. 187-211.

Impact of Non-linear Transport Properties on Low Permeability Measurements

Yuan-Yun Lin[1,2], Michael T. Myers[1]

[1]Department of Petroleum Engineering, [2] Department of Chemical and Biomolecular Engineering

University of Houston, Houston, TX 77004, USA

UNIVERSITY of HOUSTON CULLEN COLLEGE of ENGINEERING

Introduction

A significant amount of work has been recently been performed to understand the role of pore structure and mineralogy on a range of rock properties. With this in mind, an improved understanding of the transport properties in these low permeability materials is important. The Gas Research Institute (GRI) measurement protocol is the most commonly used to estimate permeability in unconventional reservoirs.

Unfortunately, the GRI measurement is unstressed and requires grinding of the samples. Both of these effects significantly alter the flow properties.

This poster discusses modeling of four different plug based measurements with differing boundary conditions, and highlights the necessity of using the full nonlinear flow equation for the interpretation of data. Our implementation, however, does not include the assumption of stress dependent constant rock compressibility and pressure dependent fluid viscosity. Ignoring the pressure dependent viscosity is consistent with modeling flow below the critical point of the flowing gas where the viscosity is relatively independent of pressure.

Due to the low flow rates encountered in these materials. We do include nonlinear flow effects of pressure dependent density and permeability, because of their large magnitude in the permeability range that we are interested (1-1000 nD).

Theory

1. Darcy's equation

For a one-dimensional, homogeneous rock, with a constant cross sectional area and fluid viscosity, the relationship between the flow and the applied pressure is given as:

$$q = -\frac{kA}{\mu}\frac{dP}{dz}$$

where q is volumetric flow rate [cm³/s], k is intrinsic permeability [Darcy], μ is fluid viscosity [cP], dP/dz is the pressure drop per unit of distance in the direction of the fluid flow [atm/cm] and A is the cross sectional area of the rock normal to the direction of fluid flow [cm²].

2. Klinkenberg correction

If slippage is considered, and the mean free path of the gas is inversely proportional to the pressure, the relation between the apparent and true permeability will be:

$$k = k_0\left(1 + \frac{b}{P}\right)$$

Where k_0 is the "Klinkenberg-corrected" permeability, b is a measure of the magnitude of the correction term due to gas slippage and P is the pressure.

3. Flow equation in porous media

We assume constant rock compressibility and fluid viscosity. Constant compressibility is consistent with moderate pore pressure changes for samples measured at higher than in situ effective stress. Viscosity is also assumed to be constant. These assumptions lead to the one dimension nonlinear equation for the flow of gas in porous media:

$$\emptyset\mu(C_\emptyset + C_f)\frac{dP}{dt} - k\frac{d^2P}{dz^2} - kC_f\left(\frac{dP}{dz}\right)^2 - \frac{dk}{dP}\left(\frac{dP}{dz}\right)^2 = 0$$

Where ϕ is porosity of porous media, μ is viscosity, C_ϕ is the rock compressibility, C_f is compressibility of the fluid, and z is the distance in the flow direction. The first two terms are the well-known diffusion equation. The nonlinear terms result from the compressibility of the gas and pressure dependent permeability (slippage effects). A correct handling of these nonlinear terms is essential for modeling the transport of gas in low permeability samples.

Steady State Modeling

The inlet and outlet pressures are held constant and the flow rate measured after the transients have relaxed. The importance of steady state is that it has a long history of use and it is experimentally simple to perform. We have used this model to evaluate our numerical technique, and the impact of early time pressure transient on the data.

$$P_{sample} = P_{initial} = 0, \quad 0 < z < L, \quad t = 0$$
$$P_{inlet} = 100, \quad z = 0, \quad t > 0$$
$$P_{outlet} = 0, \quad z = L, \quad t > 0$$

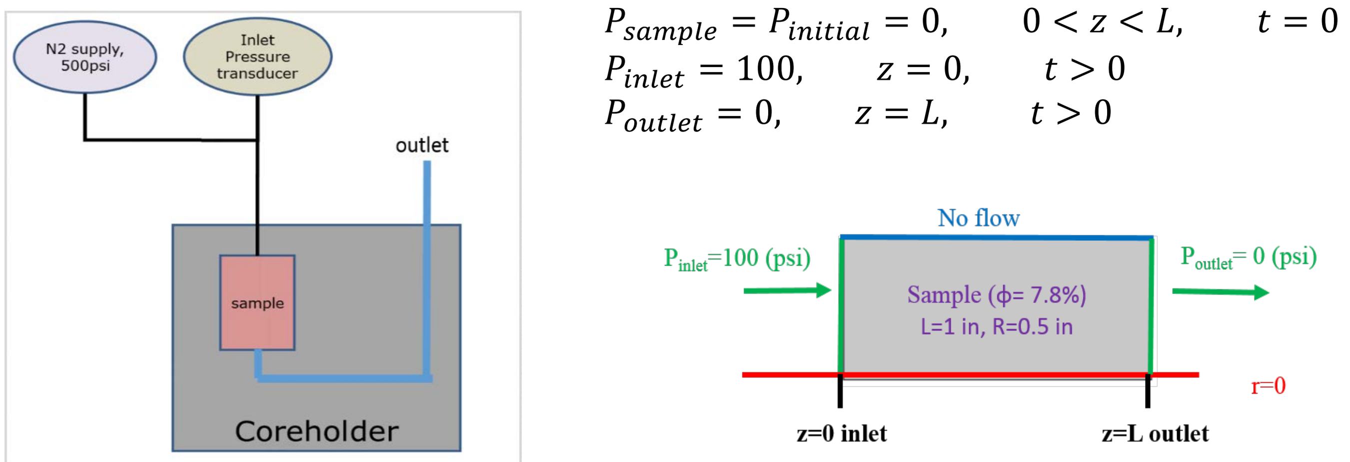

Figure 1 – (a) The block diagram for steady state permeability. (b) Exported COMSOL steady state modeling geometry. The inlet pressure is raised above ambient and vented to ambient pressure at the outlet.

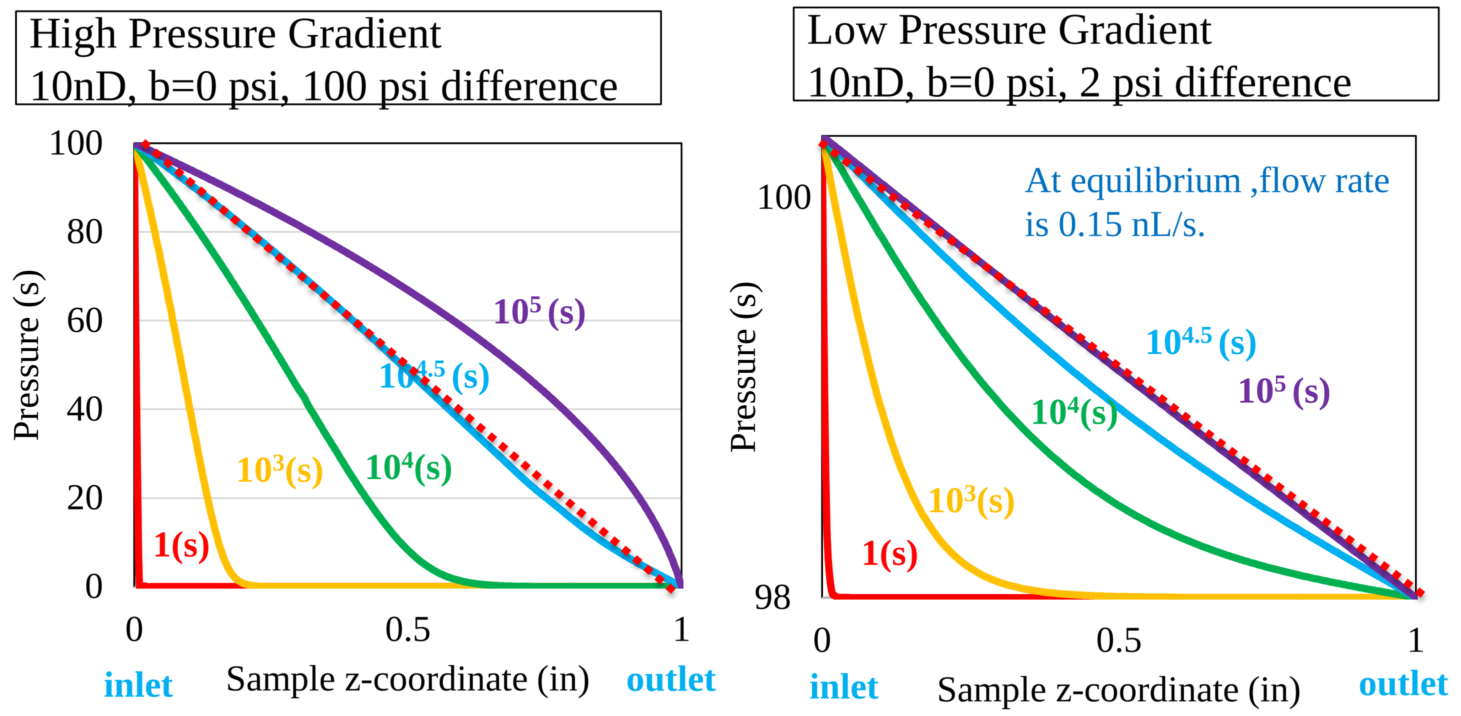

Figure 2 – The pressure profile in the sample as a function of time. One day is approximately 10^5 s. (a) For large pressure drops, a nonlinear pressure profile is observed at equilibrium . (b) For low pressure drops, the pressure profile is linear.

Inlet Flow Rate (nL/s)	4.4
Outlet Flow Rate (nL/s)	34
Calculated Permeability (nD)	9.9

Inlet Flow Rate (nL/s)	0.154
Outlet Flow Rate (nL/s)	0.157
Calculated Permeability (nD)	10.0

The permeability may be calculated for steady state measurements using the well known result for determining the pressure profile for steady state measurements:

$$k_a = \frac{2P_a\mu q_a L}{(P_1{}^2 - P_2{}^2)A}$$

Where k_a is gas permeability [Darcy], P_a is atmospheric pressure [atm], P_1 is upstream pressure [atm], P_2 is the outlet pressure [atm], L is sample length [cm], μ is gas viscosity [CP], q_a is gas flow rate at atmospheric pressure [cm³/sec], A is the cross-sectional area [cm²].

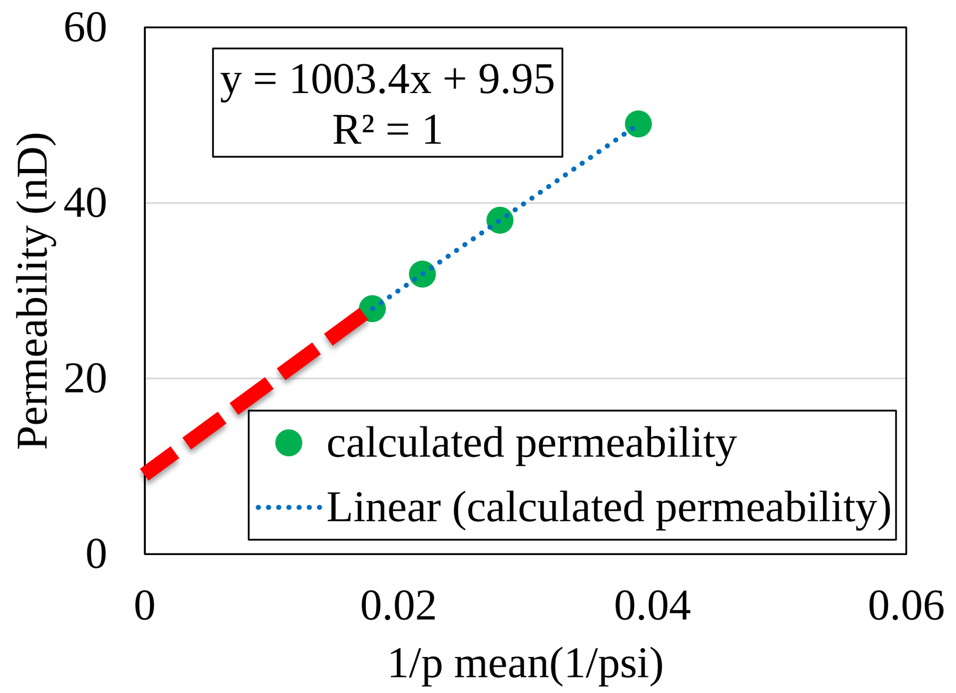

Figure 3 – Analysis of a forward modeled 10 nD sample data with 2 psi pressure difference. Darcy's equation is used to the model pressure drops and flow rates. As expected, the modeling give k_0=10 nD and b=100 psi, which are identical to the modeling input, confirming the COMSOL model calculations. The large magnitude of the correction is apparent, at low pressures this effect dominates.

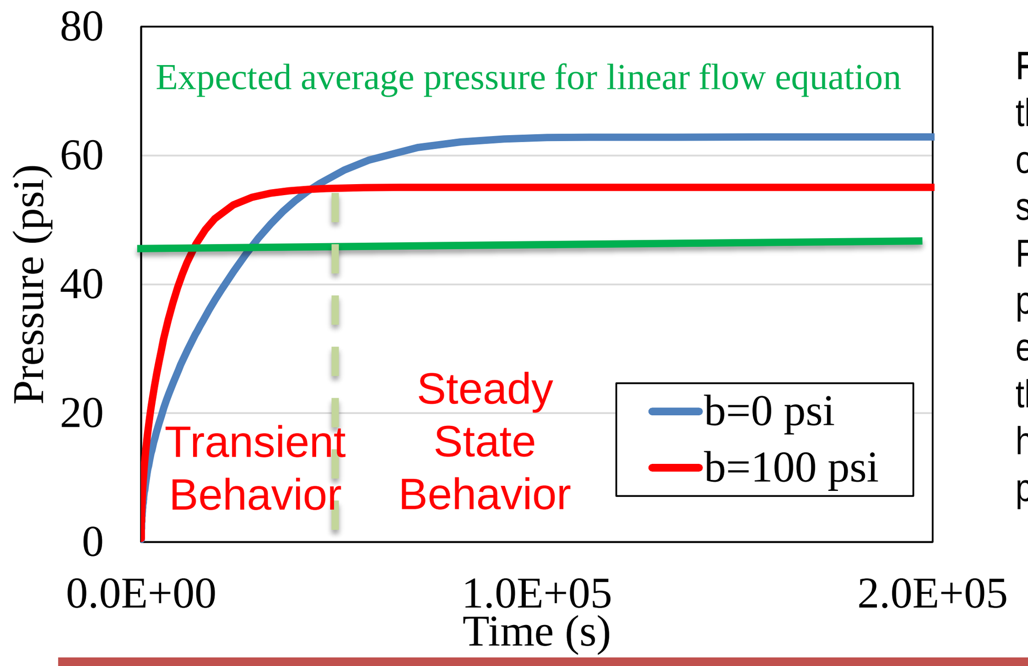

Figure 4 – The effect of the Klinkenberg correction on mean pressure for steady state modeling. For larger values of b the pressure profile equilibrates faster, and the mean pressure is higher mimicking a higher permeability.

Same Flow Rate as 10nD, b=100 psi		
Input flow rate (m/s)	Permeability, k0 (nD)	Klinkenberg factor, b (psi)
2.20 E-8	25.4	0
2.20 E-8	17.4	30
2.20 E-8	14.3	50
2.20 E-8	10	100

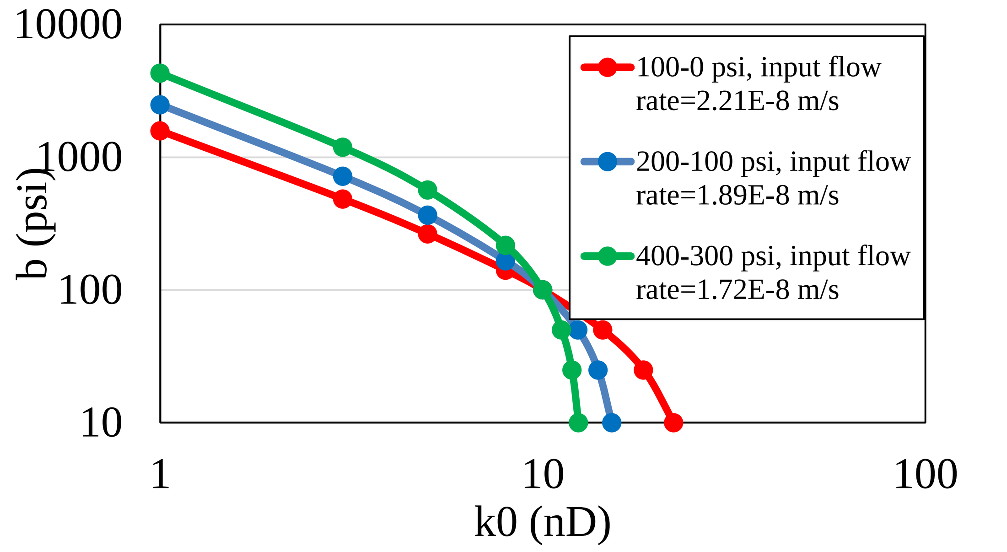

Figure 5 – Plots of the table of k0 and b for the fits. They cross at the forward modeled values of k0=10 nD and b=100 psi. This technique allows a robust determination of the parameters k0 and b. An approximate value may be obtained from the points of maximum curvature.

Unsteady State Modeling

The unsteady state permeability measurement differs from steady state by adding an upstream reference chamber (V_{up}). This reference chamber is charged to an initial pressure, then the gas are allowed to flow through the sample into ambient pressure.

$$P_{up} = 100, \quad t > 0$$
$$P_{sample} = 0, \quad 0 < z < L, \quad t = 0$$
$$P_{outlet} = 0, \quad z = L, \quad t > 0$$

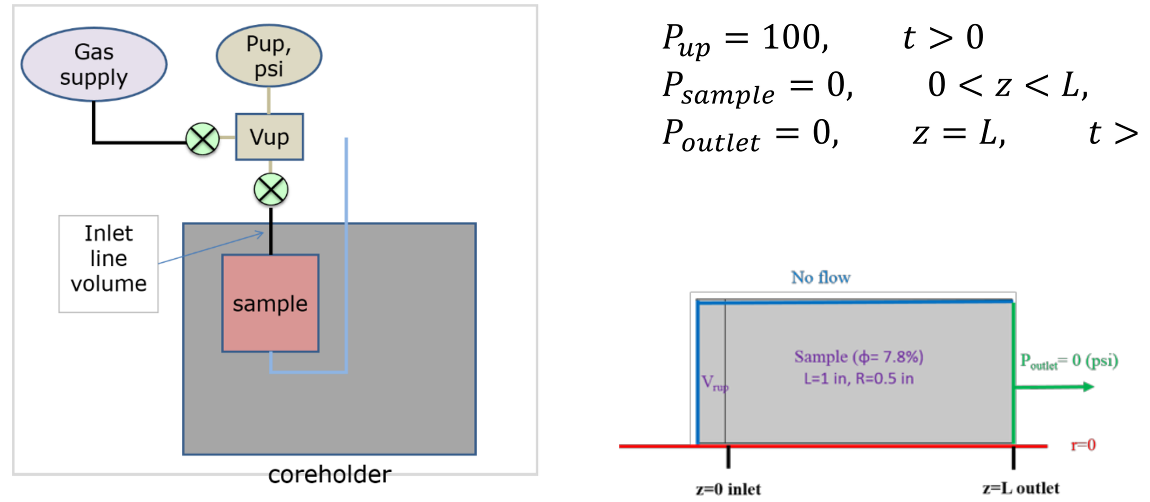

Figure 6 – (a) The block diagram for unsteady state permeability. (b) Exported COMSOL unsteady state modeling geometry. The inlet pressure is raised above ambient and vented to ambient pressure at the outlet.

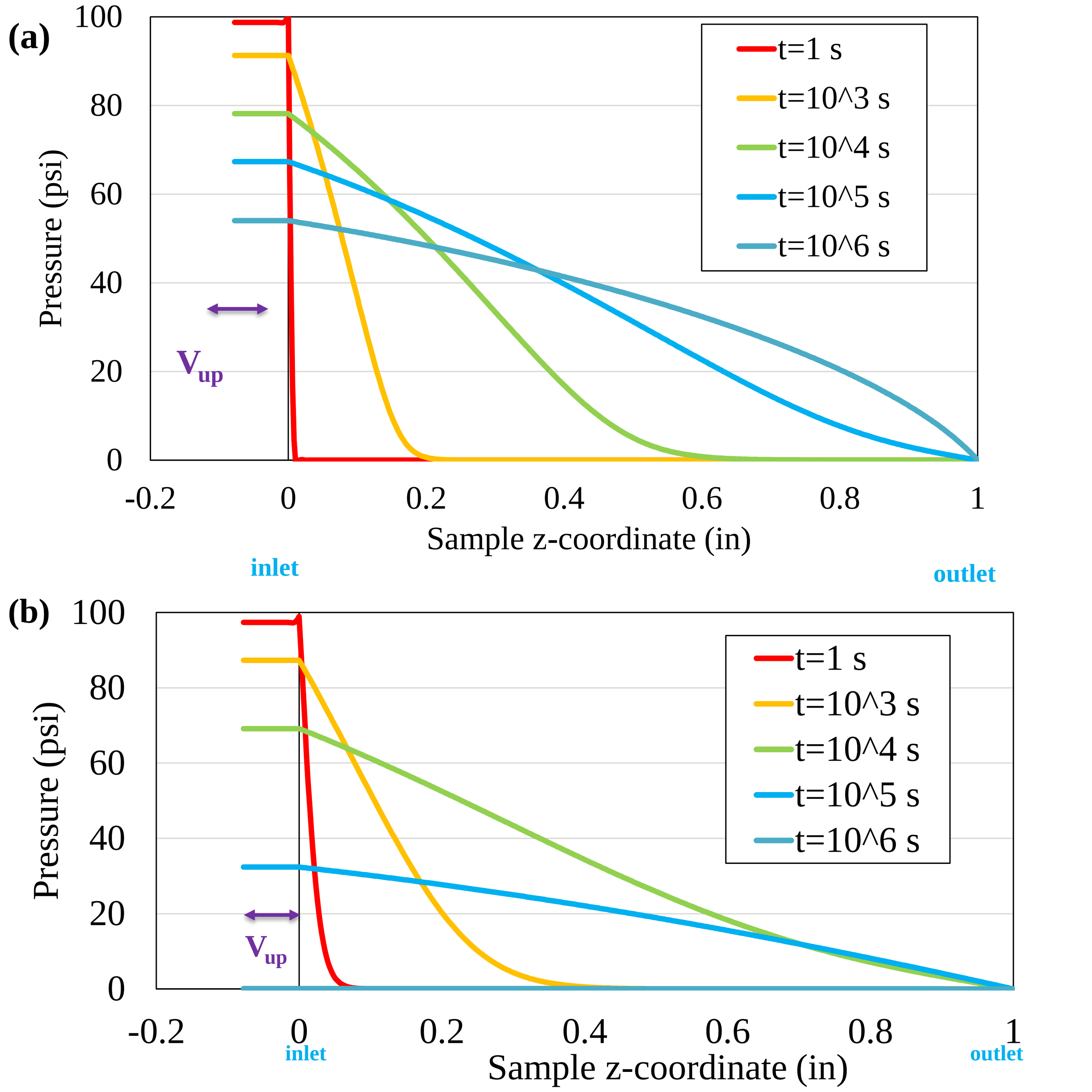

Figure 7 – The pressure profiles for the sample and the upstream chamber for the unsteady state model. (a) 10nD, b=0 psi (b) 10nD, b=100 psi. The chamber pressure to the left decreases as gas flows into the sample.

Impact of Non-linear Transport Properties on Low Permeability Measurements

Yuan-Yun Lin[1,2], Michael T. Myers[1]
[1]Department of Petroleum Engineering, [2] Department of Chemical and Biomolecular Engineering
University of Houston, Houston, TX 77004, USA

UNIVERSITY of HOUSTON
CULLEN COLLEGE of ENGINEERING

Unsteady State (Cont'd)

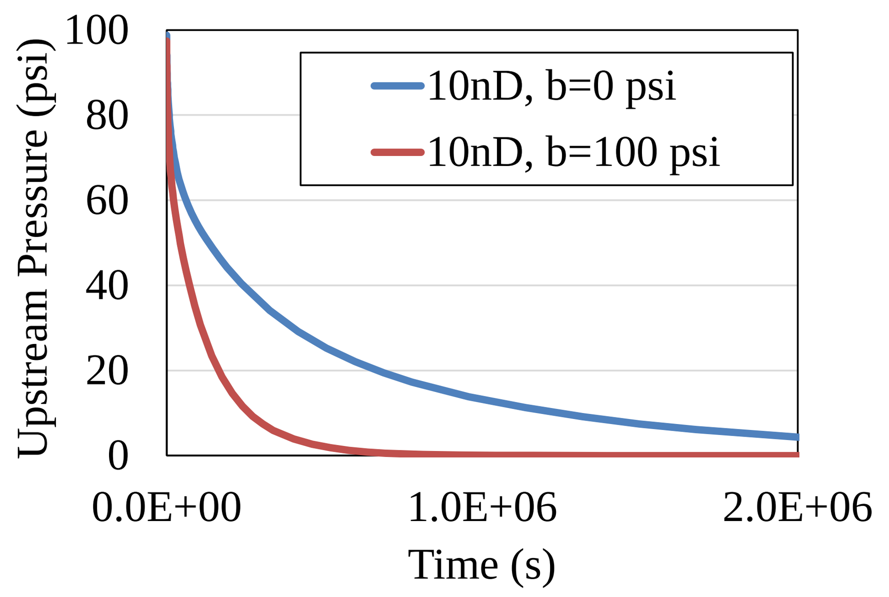

Figure 8 – The pressure profiles for b=0, 100 psi. This shows the rate of pressure decline is significantly greater when slippage is included. Tests for a 10 nanodarcy sample typically need a few days to acquire sufficient data to allow fitting for values of k0 and b.

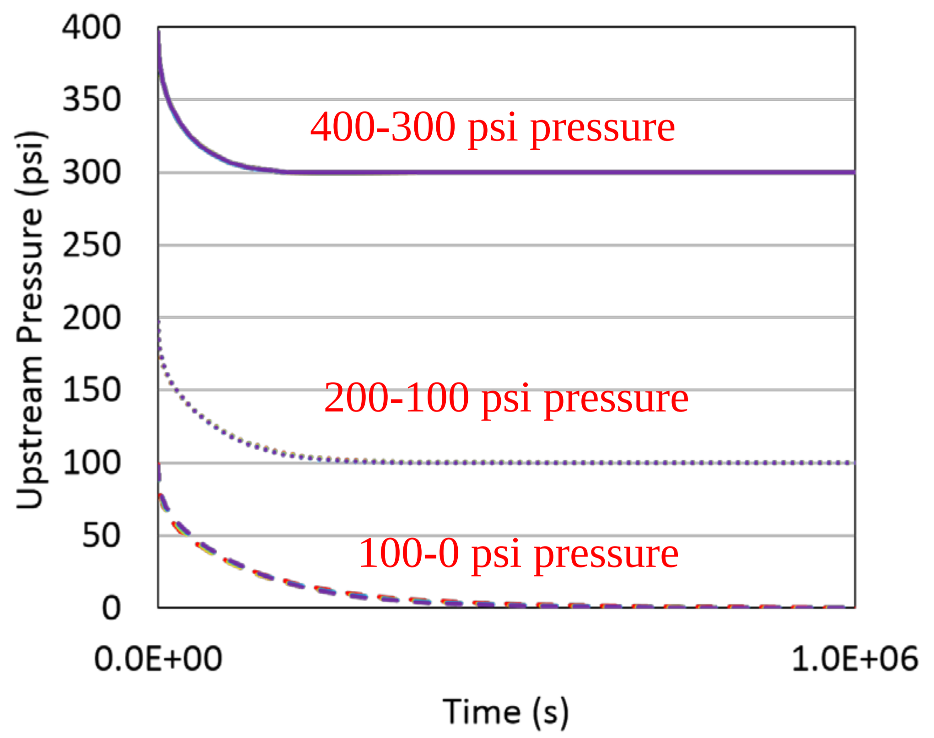

Figure 9 – Forward Modeled data for model parameters of k0=10 nD and b=100 psi. Initial upstream chamber is 100 ,200 and 400 psi, and the outlet boundary condition is 0, 100 and 300 psi. The fits for the varying values are well within experimental error. Each of the curves is the overlay of twelve different sets of parameters.

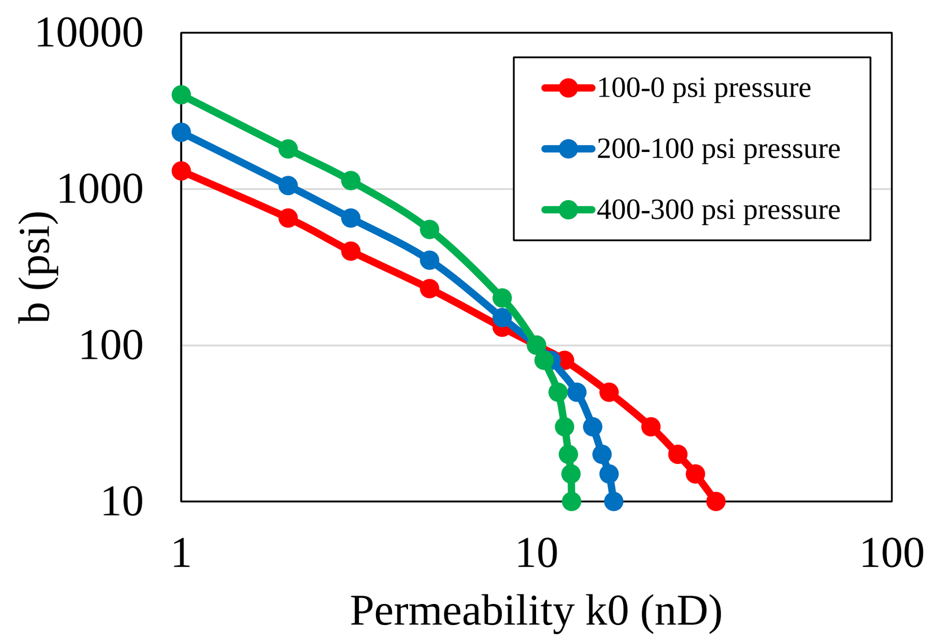

Figure 10 – The relation between k0 and b for the fits to pressure decline curves for the upstream chamber with different means stresses. The lines cross at the forward modeled values for permeability and slippage. (k=10 nD and b=100 psi).

Pulse Decay Modeling

The pulse decay permeability measurements add an additional downstream reference chamber (V_{down}). The upstream (V_{up}) and downstream chambers are charged to different pressures, which equilibrate by flow through the sample. The main advantages of this technique that the system is now closed, and mass balance is maintained. Because the chamber and pore volumes are constant, the influence of sample adsorption and diffusion affect the equilibrium pressure.

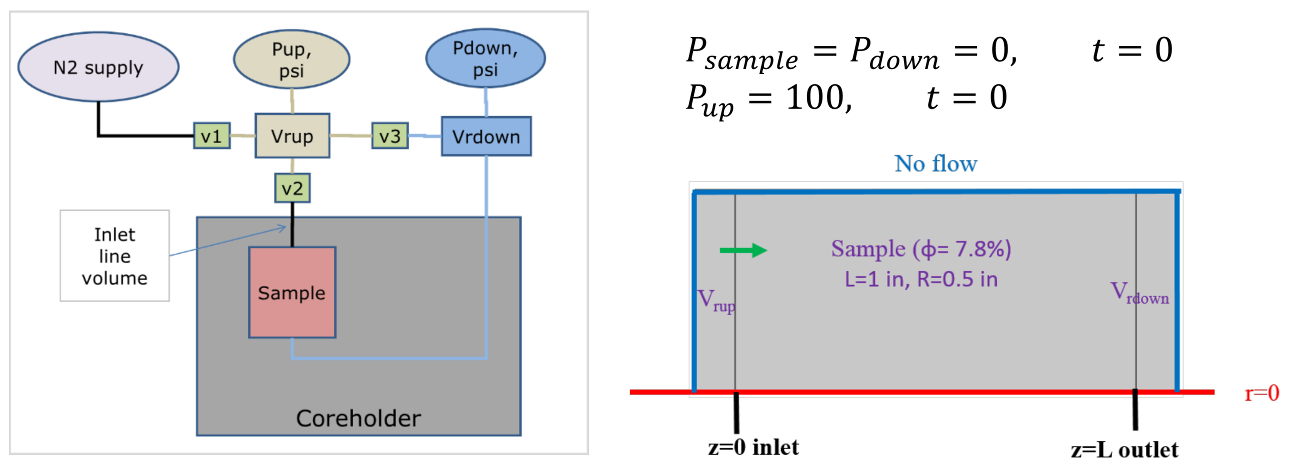

$$P_{sample} = P_{down} = 0, \quad t = 0$$
$$P_{up} = 100, \quad t = 0$$

Figure 11 – (a) The block diagram for pulse decay permeability. (b) Exported COMSOL pulse decay modeling geometry. The inlet pressure is raised above ambient and vented to ambient pressure at the outlet.

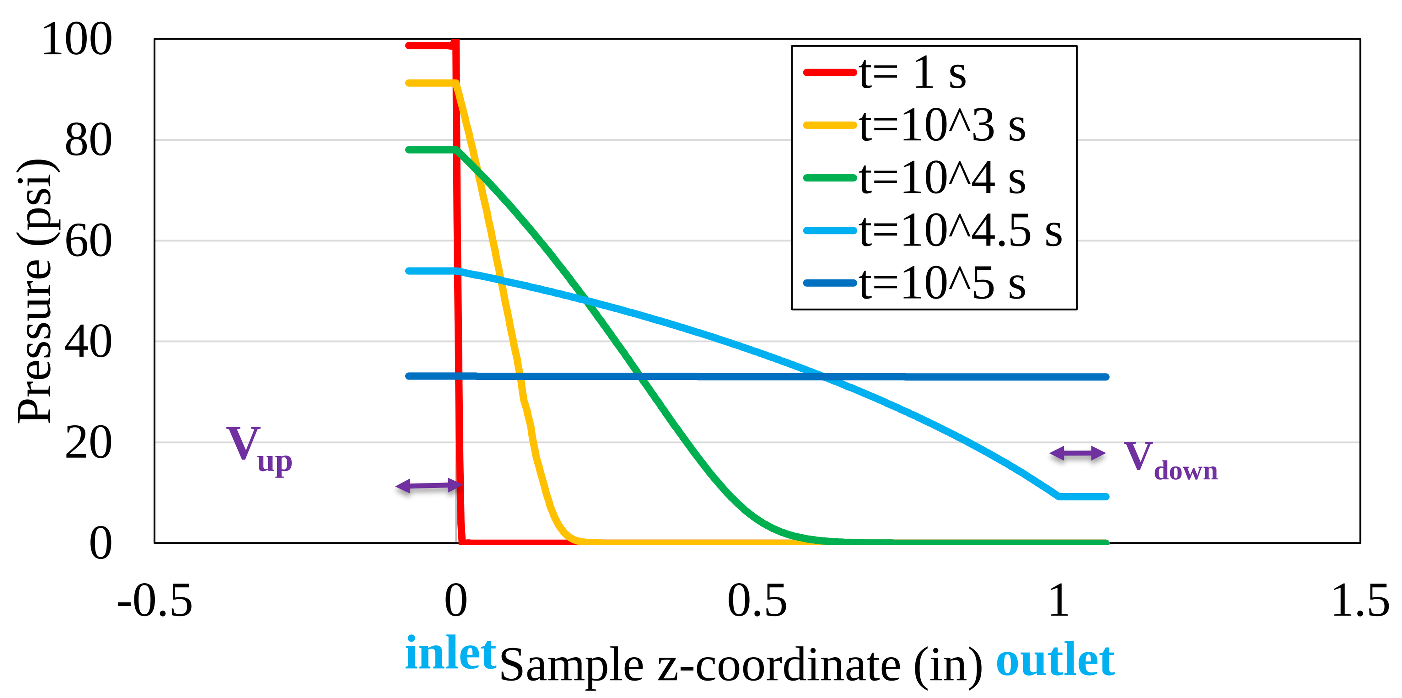

Figure 12 – The time dependent pressure profile for the pulse decay model (10nD, b=100 psi). The pressure at equilibrium is consistent with the idea gas law. The chamber and pore volumes are equal.

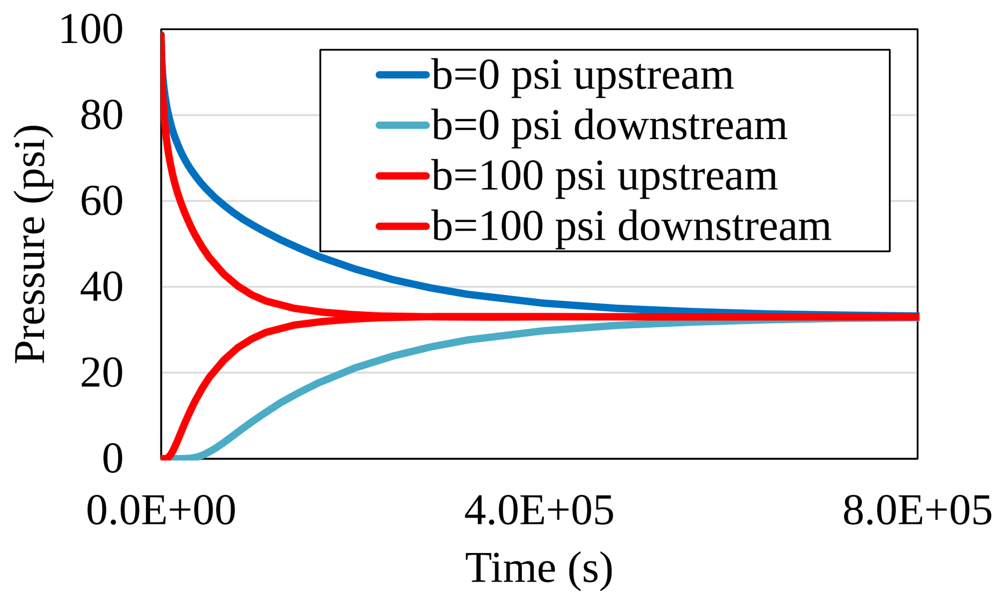

Figure 13 – Consistent with the ideal gas law, the equilibrated pressure is 33.6 psi. Differences between this modeled pressure and an experimentally measured pressure will be assumed to be due to absorption effects (no leaks). The upstream chamber and pore volume are all one cubic centimeter.

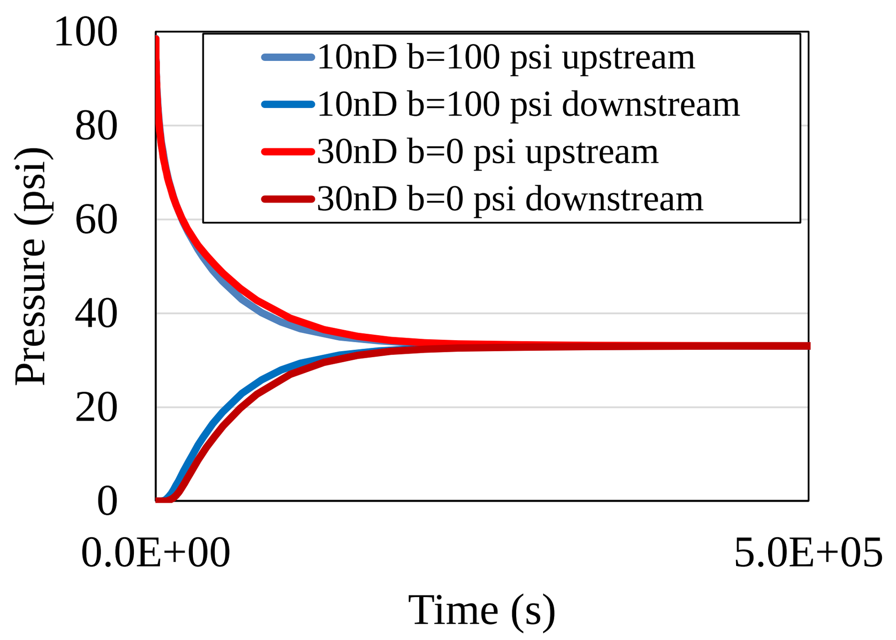

Figure 14 – The pressure profiles for 10nD b=100 psi and 30nD b=30 psi.

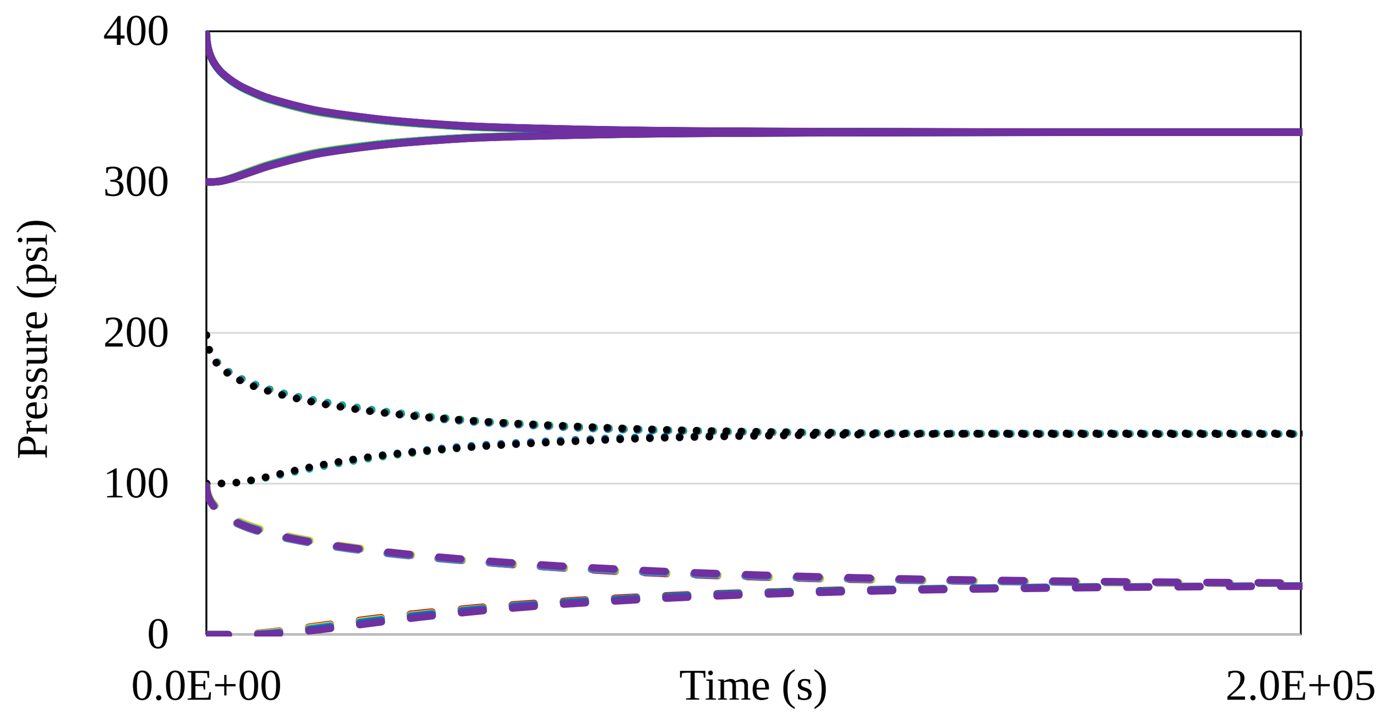

Figure 15 – The relation of k0 and b for nearly identical fits to pressure curves for the upstream chamber and downstream pressure.

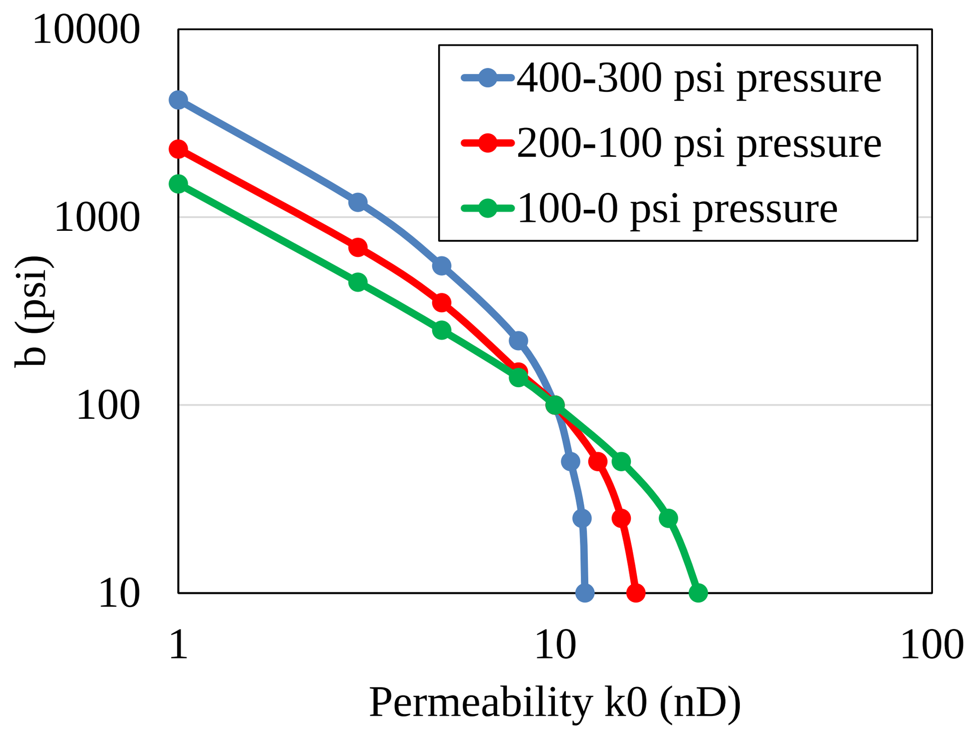

Figure 16 – The relation between k0 and b for the fits to pressure decline curves for the upstream and downstream chambers with different means stresses. The lines cross at the forward modeled values for permeability and slippage. (k=10 nD and b=100 psi).

Sinusoidal Modeling

For this model, a sinusoidal pressure is applied to the upstream reference chamber in the pulse decay apparatus. The amplitude and phase of the pressure in the downstream chamber is measured and interpreted for sample porosity and permeability. To our knowledge the only models in the literature are for interpretations of linearized flow equations.

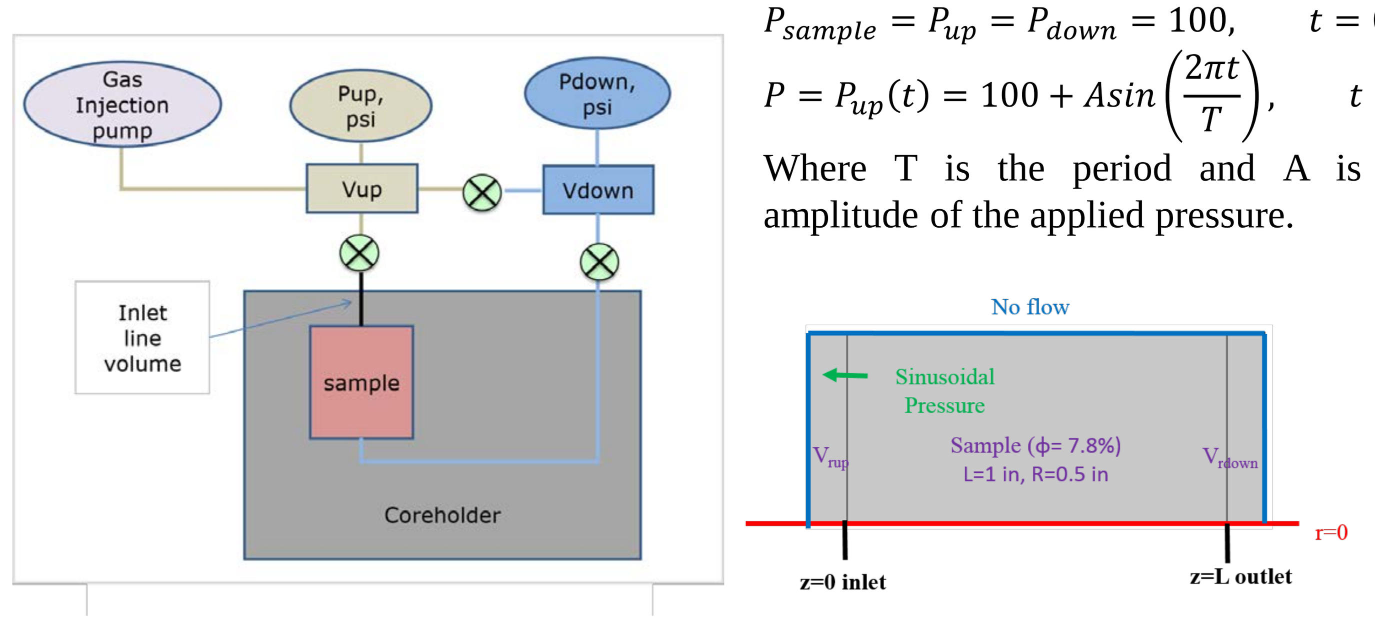

$$P_{sample} = P_{up} = P_{down} = 100, \quad t = 0$$
$$P = P_{up}(t) = 100 + A\sin\left(\frac{2\pi t}{T}\right), \quad t > 0$$

Where T is the period and A is the amplitude of the applied pressure.

Figure 17 – (a) The block diagram for sinusoidal pressure permeability. (b) Exported COMSOL sinusoidal modeling geometry. The inlet pressure is raised above ambient and vented to ambient pressure at the outlet.

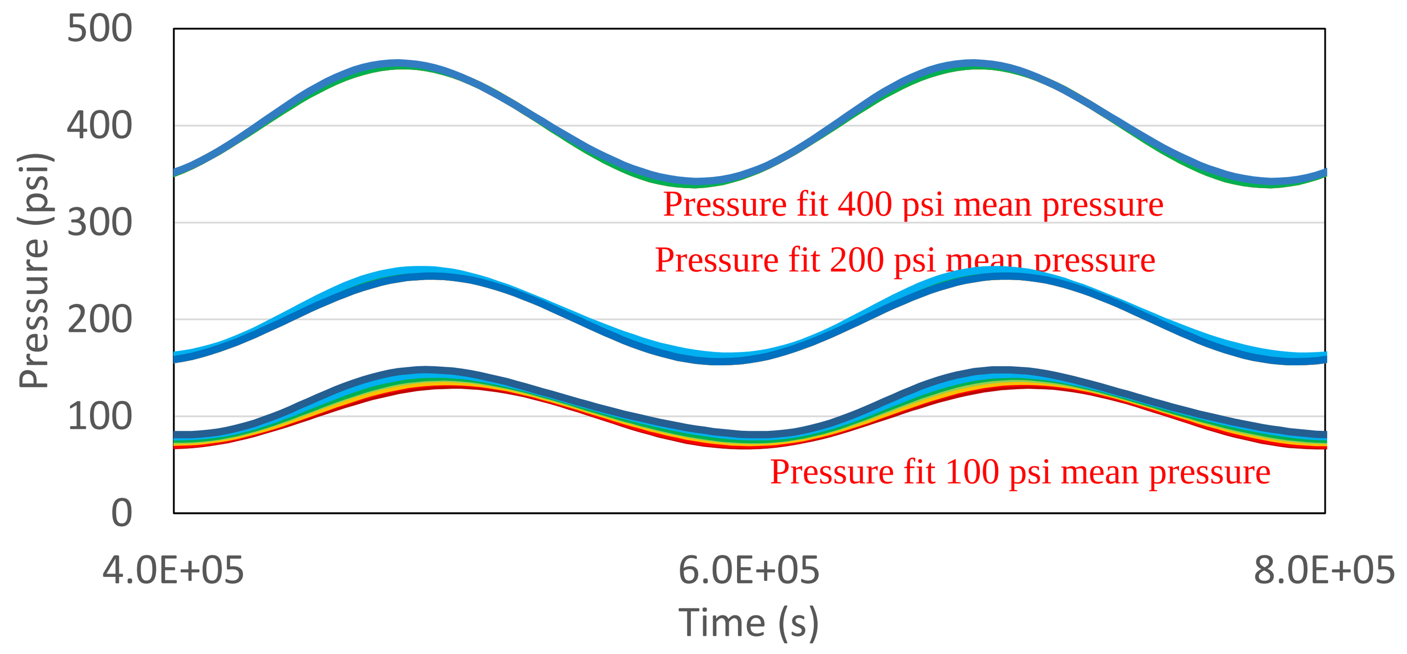

Figure 18 – The relation of k0 and b for nearly identical fits to pressure curves for the downstream pressure.

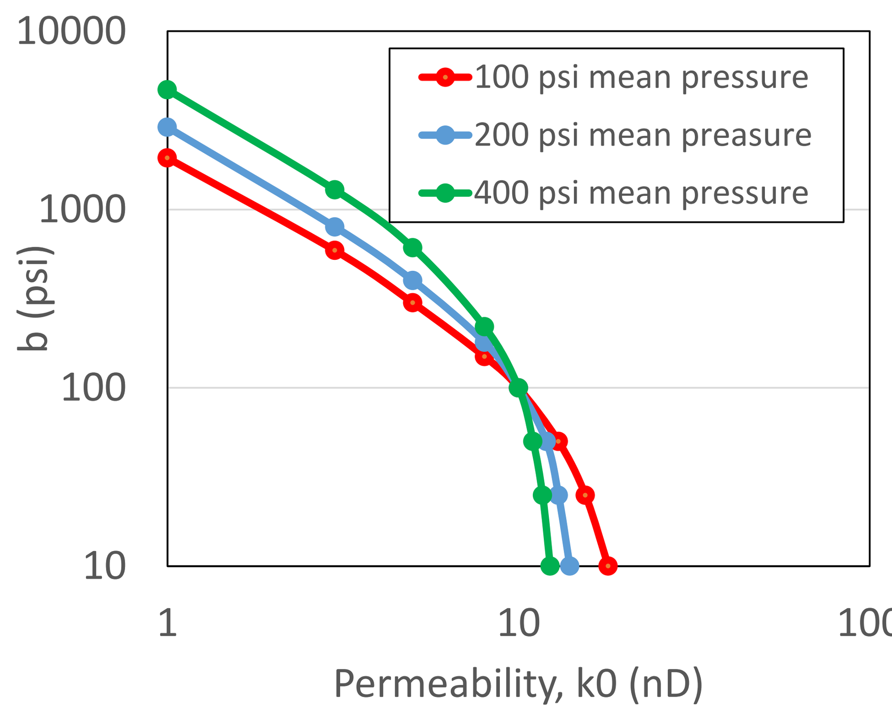

Figure 19 – The relation between k0 and b for the fits to pressure decline curves for the downstream chamber with different means stresses. The lines cross at the forward modeled values for permeability and slippage. (k=10 nD and b=100 psi).

Impact of Non-linear Transport Properties on Low Permeability Measurements

Yuan-Yun Lin[1,2], Michael T. Myers[1]

[1]Department of Petroleum Engineering, [2] Department of Chemical and Biomolecular Engineering

University of Houston, Houston, TX 77004, USA

UNIVERSITY of HOUSTON CULLEN COLLEGE of ENGINEERING

Sinusoidal Modeling (Cont'd)

Sinusoidal 1: Varying the Amplitude, No slippage

For this model, a sinusoidal pressure is applied to the upstream reference chamber in the pulse

A sinusoidal upstream pressure is applied:

$$P = 100 + A\sin\left(\frac{2\pi t}{T}\right), \quad T = 200{,}000\ \text{sec}, \quad k_0 = 10nD, \quad b = 0\ psi$$

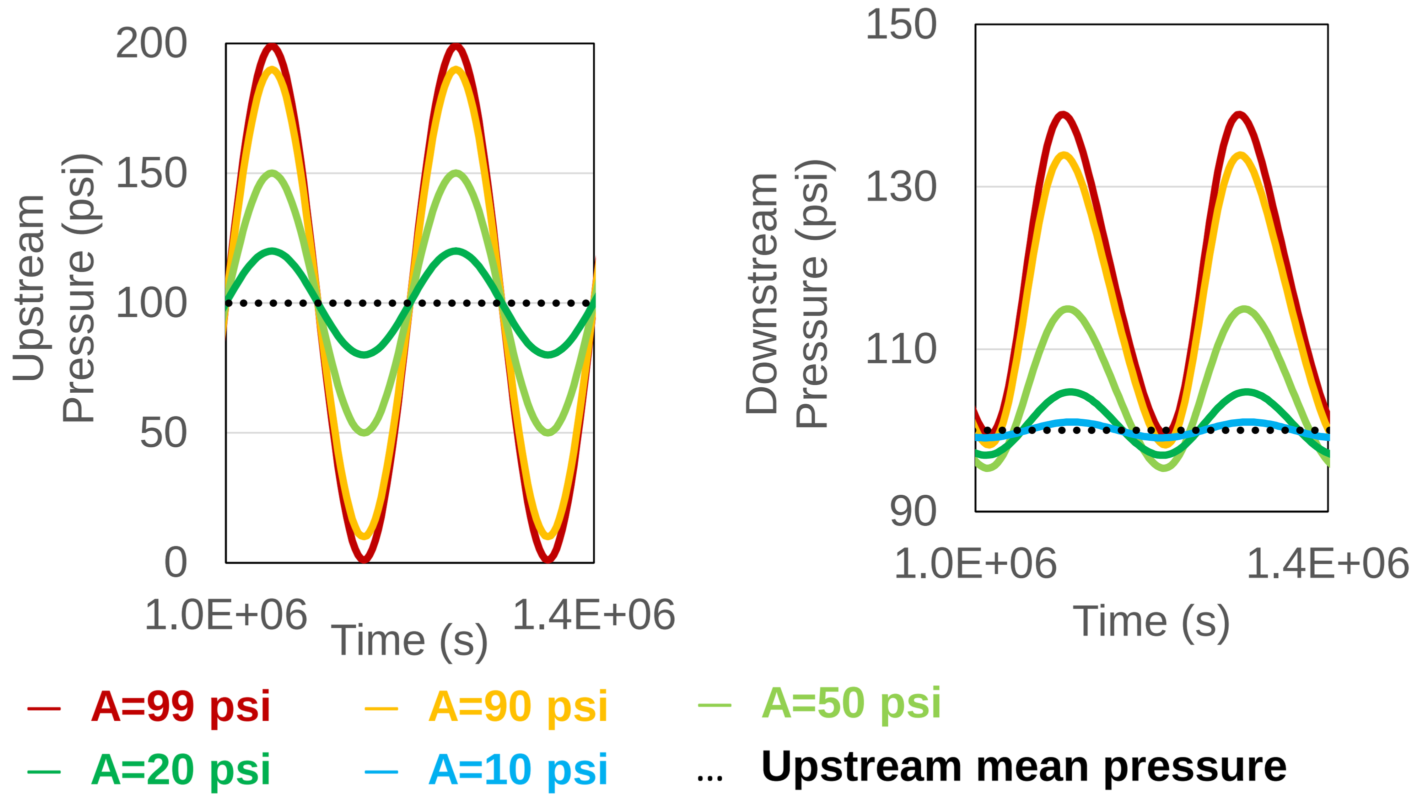

Figure 20 – The time dependent downstream pressure as a function of varying the amplitude of the upstream pressure. The average upstream pressure is constant. The average downstream pressure increases with increasing amplitude of the upstream pressure. This is a result of the nonlinear pressure dependent density effect.

Fourier series analysis allow a periodic function to be decomposed into a sum of simple sine waves. We make use of Fourier transform to quantify the magnitude of the nonlinear effects on the transport of gas as measured by the sinusoidal permeability measurement protocol.

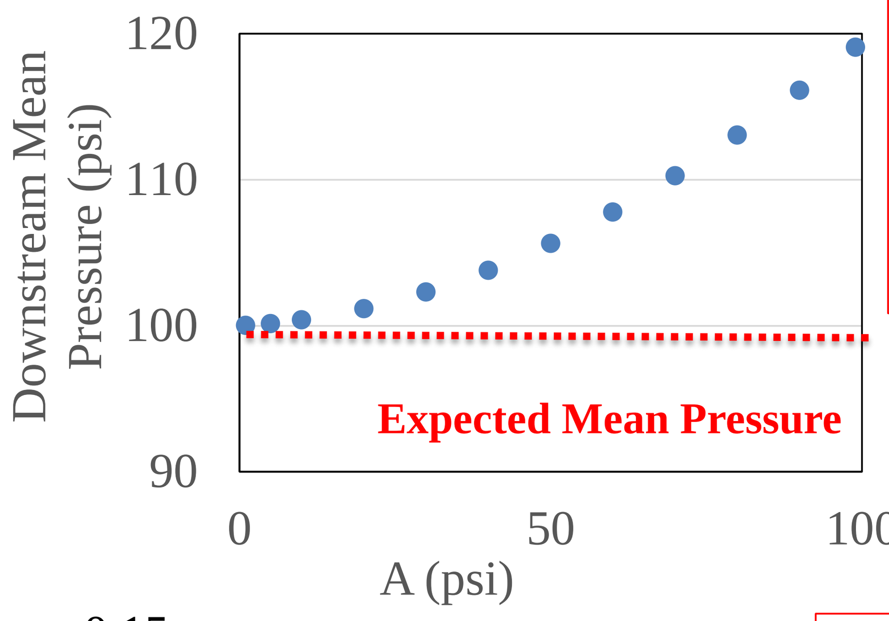

Figure 21 – The mean downstream pressure increases as the upstream pressure amplitude increases.

The total harmonic distortion, or THD, of a signal is a measurement of the harmonic distortion present and is defined as the ratio of the sum of the powers of all harmonic components to the power of the fundamental frequency.

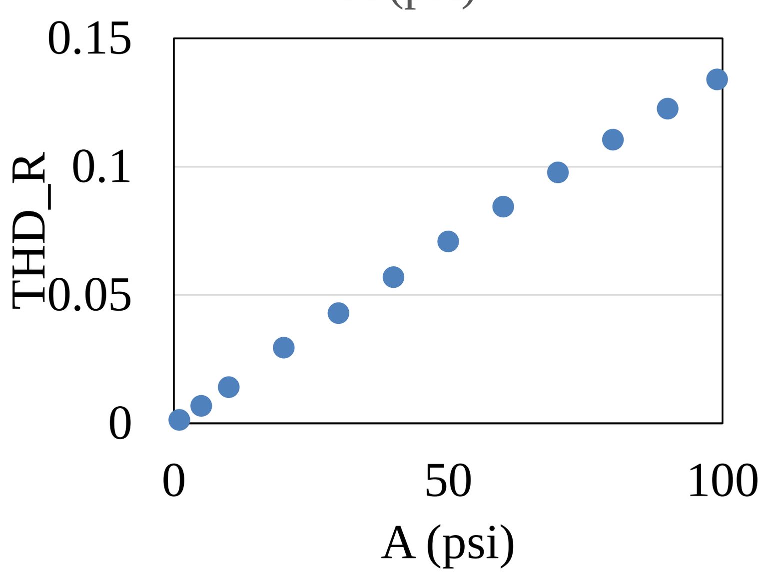

Figure 22 – The total harmonic distortion (THD) result of models with different upstream pressure amplitude. As the amplitude increase, the THD increases.

Sinusoidal 2: Varying k0, No slippage

In the following models, only the permeability is changed.

$$P = 100 + 90\sin\left(\frac{2\pi t}{T}\right), \quad T = 200{,}000\ \text{sec}, \quad different\ k_0, \quad b = 0\ psi$$

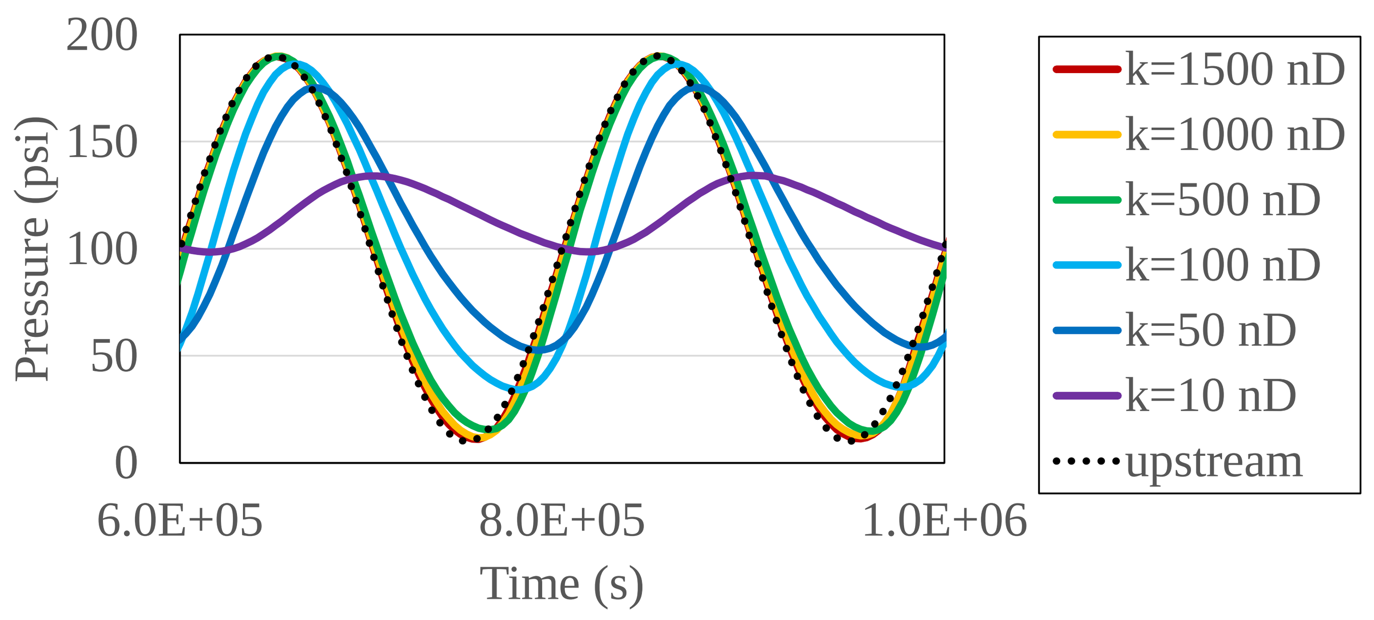

Figure 23 – The downstream pressure as a function of permeability with no gas slippage. The amplitude increases and phase difference decreases as the permeability increases. The model exhibits increasingly linear behavior with increasing permeability.

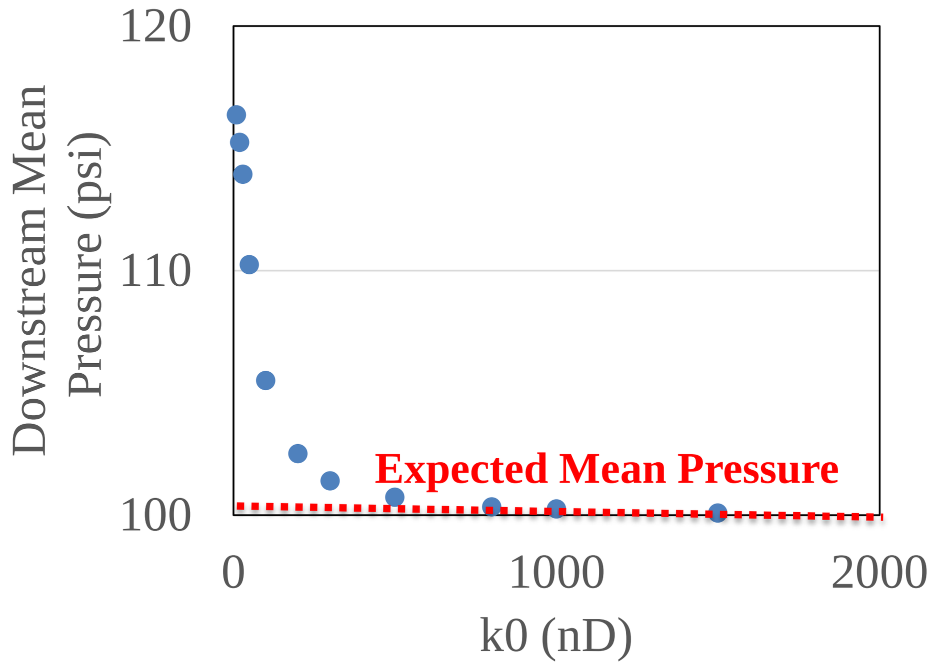

Figure 24 – The mean pressure of downstream pressure decreases as the sample permeability increases.

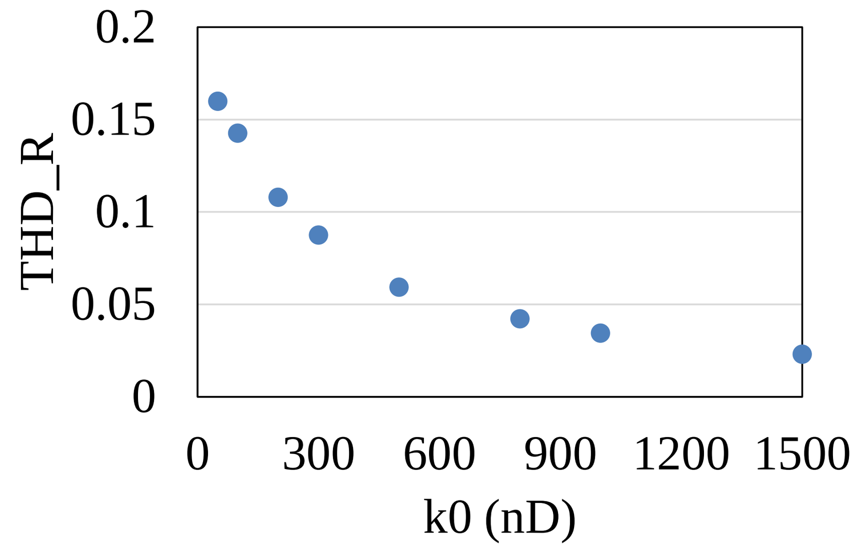

Figure 25 – The total harmonic distortion (THD) result of models with different permeability. As the permeability increase, the THD decreases.

Sinusoidal 3: With Slippage

In the following models, different gas slippage effect are discussed.

$$P = 100 + 90\sin\left(\frac{2\pi t}{T}\right), \quad T = 200{,}000\ \text{sec}, \quad k_0 = 10\ nD, \quad different\ of\ b$$

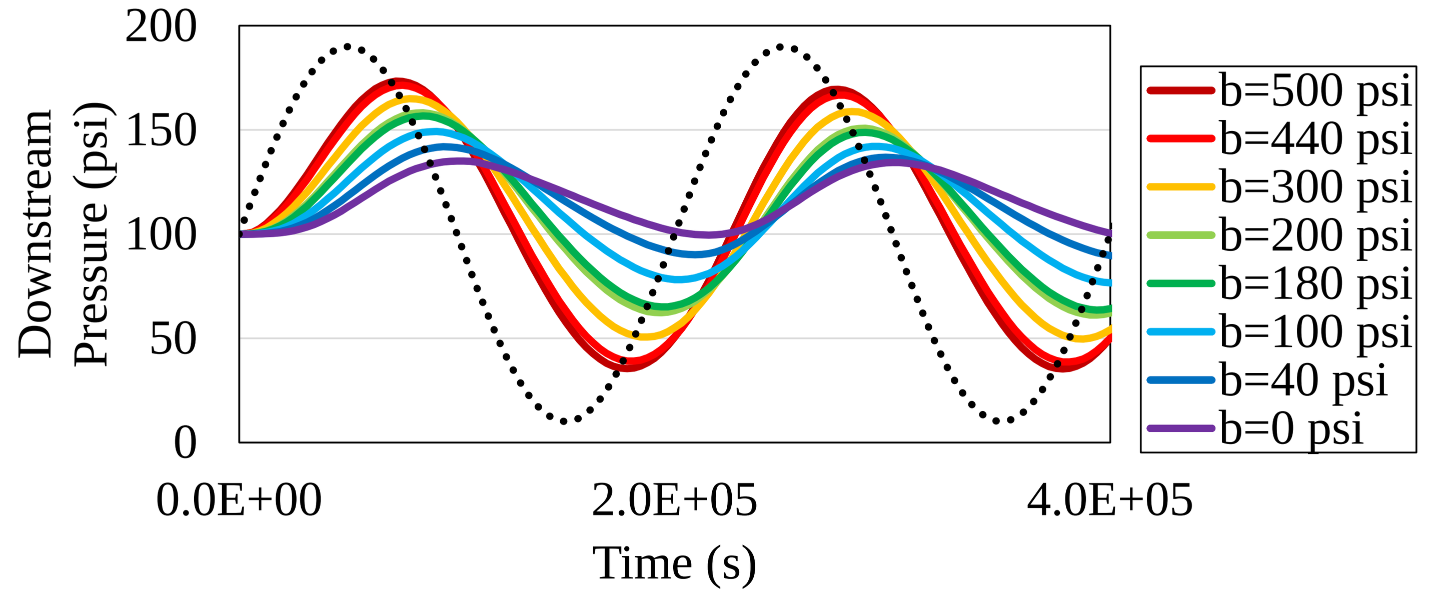

Figure 26 – The pressure of the downstream chamber under different Klinkenberg corrections. The value of the average pressure results from a competition between the pressure dependent density and the effects of gas slippage.

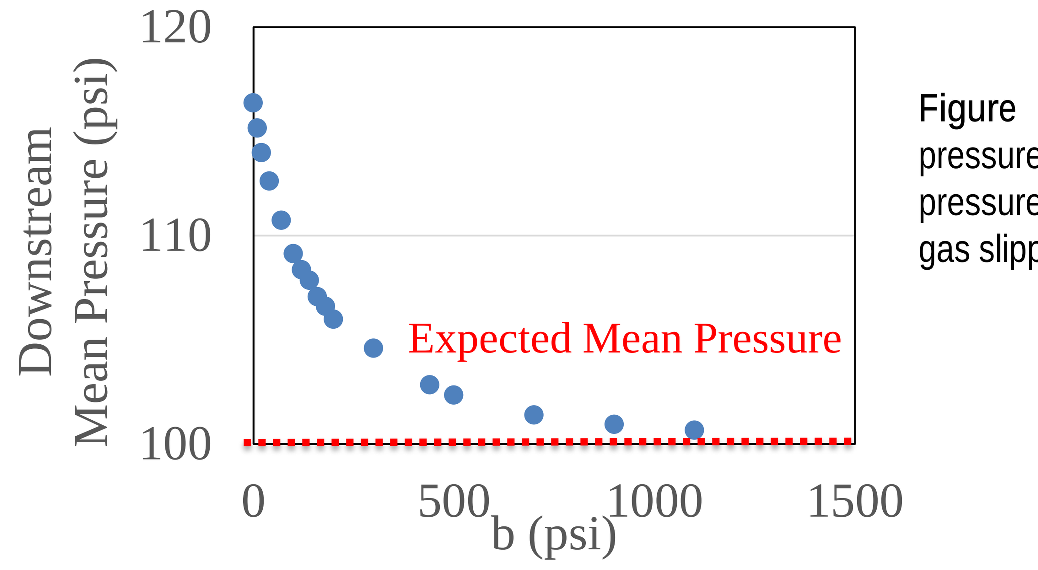

Figure 27 – The mean pressure of downstream pressure decreases as the gas slippage effect increases.

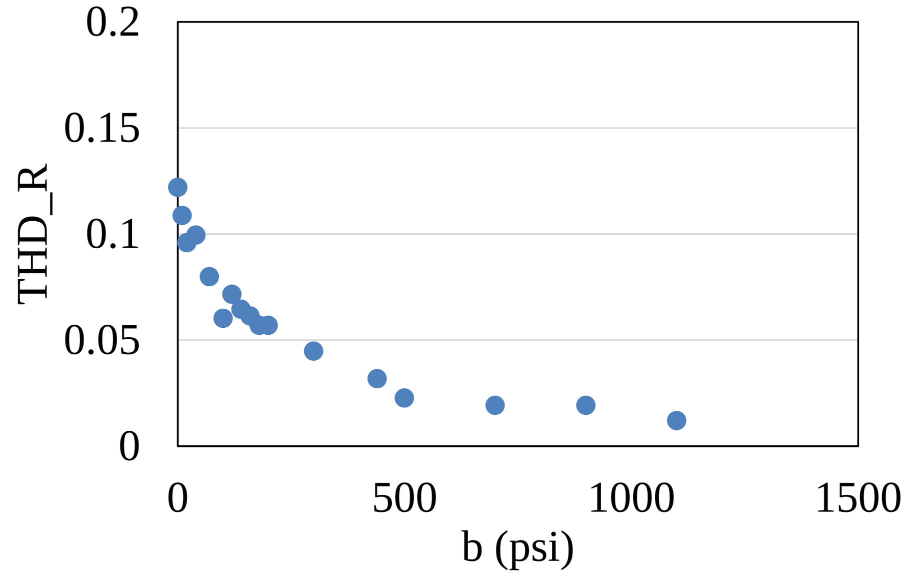

Figure 28 – The THD result of different gas slippage model. As the b increases, the THD result decreases.

Conclusions

The computations performed for a typical model in this study take only a few minutes on a desk top computer. The goal of the work is to extract the parameters k_0 and b from measured chamber pressure data by comparison to COMSOL Multiphysics™ models. This is performed by embedding and fitting the COMSOL model as the kernel in a nonlinear fitting routine and fitting k0 and b as discussed. This sort of parameter extraction typically requires at most a few hours of computation time and is well within the capabilities of most desktop computers.

We have developed models for a variety of geometries and experimental protocols:

- Steady State: Historically the most widely used technique for measuring permeability. For low permeability samples, there are nonlinearities that must be taken into account to accurately analyze the data for k_0 and b. To acquire data that allows a linearized version of the equation, the flow rates are too low to be reliably measured.
- Unsteady State: This technique takes the least time to perform the measurement over a wide range of flow rates. At low permeabilities the full nonlinear equation must be used to extract the correct value of k_0 and b. Measurements at two or more mean stresses are required to allow unambiguous extraction of the transport parameters. The measurement time is comparable to many other petrophysical measurements (days). This technique should become the standard for low permeability plug measurements.
- Pulse Decay: The measurement provides mass balance which allows the effects of absorption and adsorption to be included in models. This makes it the most robust measurement for determining all the physical mechanisms, but small leaks would negate these advantages. Similar to unsteady state measurements at several means stresses should be made.
- Sinusoidal: Nonlinearities can be easily quantified through the use of Fourier analysis. The pressure dependent density introduces harmonic distortion. Addition of gas slippage reduces this effect. In particular the average pressure in the outlet chamber is higher than the average pressure in the inlet chamber due to the pressure dependent density. The analogue of optical rectification in nonlinear optics. Fourier analysis of the data in the downstream chamber allow the nonlinear effects to be quantified.

Future work will include modeling the effects of anisotropic samples, gas sorption and diffusion effects, and comparing models to transport data. We will also include pressure dependent viscosities to model the effect of flowing gas above the critical point.

References

- Cui, X., A. M. M. Bustin, and Robert M. Bustin. "Measurements of gas permeability and diffusivity of tight reservoir rocks: different approaches and their applications." Geofluids 9.3 (2009): 208-223.
- Sander, Regina, Zhejun Pan, and Luke D. Connell. "Laboratory measurement of low permeability unconventional gas reservoir rocks: A review of experimental methods." Journal of Natural Gas Science and Engineering 37 (2017): 248-279.
- Darcy, Henry. Les fontaines publiques de la ville de Dijon: exposition et application... Victor Dalmont, 1856.
- Klinkenberg, L. J. "The permeability of porous media to liquids and gases." Drilling and production practice. American Petroleum Institute, 1941.
- Aronofsky, J. S. "Effect of gas slip on unsteady flow of gas through porous media." journal of Applied Physics 25.1 (1954): 48-53.
- Profice, Sandra, et al. "Permeability, porosity and klinkenberg coefficien determination on crushed porous media." Petrophysics 53.06 (2012): 430-438
- Fischer, G. J. "The determination of permeability and storage capacity: Pore pressure oscillation method." International Geophysics Series 51 (1992): 187-187.